On the Theoretical Calculation of Friction Factors for Laminar, Transitional, and Turbulent Flow of Newtonian Fluids in Pipes and Between Parallel Plane Walls

RICHARD W. HANKS

General Electric Company, Richland, Washington

Various modifications of the Prandtl mixing-length model for turbulent momentum transport in pipes and between parallel plane walls are discussed. The most complete modification, due to Gill and Scher, is improved by replacing one of their two empirical constants by a theoretically calculable parameter. The new theory is compared with experimental data from the literature and found to reproduce frictional resistance data accurately for all values of the Reynolds number. It is somewhat in error for velocity profiles at high Reynolds numbers, but accurately reproduces velocity profile data in the transition region. The new theory represents the first accurate semi-theoretical calculation of frictional resistance coefficients for all regimes of flow (laminar, transitional, and turbulent) for both pipes and parallel plane ducts, and of velocity profiles in the transitional flow regime in either geometry.

Since the introduction of the concept of a mixing length by Prandtl (*1*) various researchers (*2* to *5*) have attempted to develop analytical expressions for the velocity profile for Newtonian fluids undergoing turbulent flow in straight channels of constant cross section. These modifications of the original theory have each included many of the effects ignored by Prandtl.

Prandtl (*1*) ignored the spatial variation of shear stress, the molecular momentum flux, and the viscous damping effect of the wall on the eddy properties of the flow near the wall. Van Driest (*4*) introduced an exponential factor into the expression for the mixing length to account for the damping influence of the wall on the eddies, and included the molecular flux. Gill and Scher (*5*) modified the Van Driest viscous damping term and introduced the shear-stress variation across the conduit. In addition to the advantage of a continuous velocity profile expression, such as developed by Van Driest (*4*), the Gill and Scher modification (*5*) caused the velocity gradient to vanish at the duct centerline, a feature different from all previous workers' results.

The present work was undertaken to improve the usefulness of the Gill and Scher modification for engineering calculations for the transition flow regime. In their work, Gill and Scher (*5*) used Van Driests' (*4*) exponential damping term and introduced an additional empirical constant in an attempt to include flows in the transition region. They used the same two empirical constants for both flow in pipes and between parallel plates. As will be shown, one of these empirical constants can be replaced by a theoretically calculable parameter, thus reducing the number of empirical constants to one and achieving much better agreement between the theoretical and experimental values of friction factors and Reynolds numbers.

REVIEW OF PREVIOUS WORK

The time-averaged momentum flux, $\bar{\tau}_{ij}$, for turbulent flow may be thought of (*6*) as composed of two parts: a molecular flux, $\tau_{ij}^{(l)}$, and a turbulent flux, $\tau_{ij}^{(t)}$. This latter flux is often called the Reynolds stress. Prandtl proposed (*1*) that $\tau_{ij}^{(t)}$ be expressed as

$$\tau_{ij}^{(t)} = \rho L^2 \left(-\frac{\partial v_i}{\partial x_j}\right)^2 \tag{1}$$

where L is the so-called "mixing-length," which was related to position by $L = ky$, where k was a universal constant and y is distance measured from the duct boundary. Van Driest (*4*) introduced an exponential damping term into the definition of L as follows:

$$L = ky\,[1 - \exp\,(-\phi y/y_m)] \tag{2}$$

where y_m is the maximum value of y, and ϕ is a constant related to the Reynolds number. Gill and Scher (*5*) modified Van Driest's definition of ϕ by introducing the empirical parameter a to give

$$\phi = \frac{N_{Re}{}^* - a}{b} \tag{3}$$

In Equation (3) $N_{Re}{}^*$ is a Reynolds number defined as

$$N_{Re}{}^* = y_m u^* \;\; \rho/\mu \tag{4}$$

and $u^* = (\tau_w/\rho)^{1/2}$ is the familiar friction velocity. In Equation (3) the empirical parameter a reflects (*5*) the departure of the flow from the critical transition Reynolds number and b is an empirical parameter which is essentially the same as Van Driest's and which accounts for the depth of penetration of the viscous wall damping effect into the stream. Gill and Scher used the empirical values $a = 60$ and $b = 22$ for both flow in pipes and between parallel plates. In the following paragraphs these two flow systems are reanalyzed by using Equation (2) for L and replacing a in Equation (3) by a theoretically calculable parameter. Some significant features of the theory which were not made clear by Gill and Scher are also discussed.

THEORETICAL ANALYSIS

Pipe Flow Case

In terms of the dimensionless position variable, $\xi = r/r_w$, Equations (1) and (2) can be combined with the

Richard W. Hanks is with Brigham Young University, Provo, Utah.

usual definition of the Newtonian molecular momentum flux and the solution of the time-averaged equation of motion (6) to obtain the following dimensionless expression for the total momentum flux:

$$0 = -\xi + \frac{1}{N_{Re}^*}\left(-\frac{du^+}{d\xi}\right) + k^2(1-\xi)^2\{1-\exp[-\phi(1-\xi)]\}^2\left(-\frac{du^+}{d\xi}\right)^2 \tag{5}$$

in which $u^+ = v(\xi)/u^*$. In view of Equation (3), N_{Re}^* is seen to be a unique parameter such that its specification in Equation (5) completely determines the velocity profile. For purposes of computation, however, a and b in Equation (3) must be specified. This is more conveniently accomplished if N_{Re}^* is replaced by a slightly different parameter. From the conventional definitions of the Fanning friction factor and Reynolds number, it is easy to show that

$$N_{Re}^* = \frac{1}{4}R\sqrt{2} \tag{6}$$

$$R \equiv N_{Re}\sqrt{f} \tag{7}$$

Consequently, Equations (3) and (5) become, respectively

$$\phi = \frac{R - R_c}{2b\sqrt{2}} \tag{8}$$

and

$$0 = -\xi + \frac{2\sqrt{2}}{R}\left(-\frac{du^+}{d\xi}\right) + k^2(1-\xi)^2\{1-\exp[-\phi(1-\xi)]\}^2\left(-\frac{du^+}{d\xi}\right)^2 \tag{9}$$

In Equation (8) the term R_c is used to replace the a of Equation (3) because it is recognized that a really represents the critical laminar-turbulent transitional value of R. In Equation (9), when $R = R_c$, the term involving ϕ vanishes, corresponding to the laminar-turbulent transition.

For Newtonian flow in pipes, it is well known (7) that $(N_{Re})_c = 2{,}100$, for which case Equation (7) gives

$$R_c = 2{,}100\sqrt{16/2{,}100} = 183.303 \tag{10}$$

This critical value of N_{Re} is the basis of a theory (7) which will be used to calculate R_c for the parallel plate case below. It is of interest to note that choosing $a = 60$ corresponds to setting $R_c = 169.705$ and $(N_{Re})_c = 1{,}800$. This value of the critical Reynolds number is at variance with accepted results (7).

As Gill and Scher (5) observed in their analysis, Equation (9) is a simple quadratic in $(-du^+/d\xi)$ and is easily solved formally to obtain

$$u^+ = \frac{\sqrt{2}}{k^2R}\int_\xi^1 g(k, R, \phi, \xi')d\xi' \tag{11}$$

where

$$g(k, R, \phi, \xi) = \frac{\left\{1 + \frac{1}{2}k^2R^2\xi(1-\xi)^2[1-\exp(-\phi(1-\xi))]^2\right\}^{1/2} - 1}{(1-\xi)^2[1-\exp(-\phi(1-\xi))]^2} \tag{12}$$

The mean velocity $<v>$, is given by $2u^*\int_0^1 \xi u^+ \, d\xi$. From the definitions of u^*, f, and R, it therefore follows that

$$N_{Re} = \frac{2}{k^2}\int_0^1 \xi \int_\xi^1 g(k, R, \phi, \xi')d\xi' \, d\xi \tag{13}$$

The velocity profile may be expressed in dimensionless form as

$$v(\xi)/<v> = \frac{1}{2}\frac{\int_\xi^1 g(k, R, \phi, \xi')d\xi'}{\int_0^1 \xi \int_\xi^1 g(k, R, \phi, \xi')d\xi' \, d\xi} \tag{14}$$

and the ratio of average to maximum velocity is given by

$$<v>/v_{\max} = 2\frac{\int_0^1 \xi \int_\xi^1 g(k, R, \phi, \xi')d\xi' \, d\xi}{\int_0^1 g(k, R, \phi, \xi)d\xi} \tag{15}$$

Flow Between Parallel Planes

For the flow of an incompressible Newtonian fluid between infinite parallel planes separated by a distance $2h$, the dimensionless expression for the total momentum flux may be written for the present model of the Reynolds stress as

$$0 = -\xi + \frac{4\sqrt{2}}{R}\left(-\frac{du^+}{d\xi}\right) + k^2(1-\xi)^2\{1-\exp[-\phi(1-\xi)]\}^2\left(-\frac{du^+}{d\xi}\right)^2 \tag{16}$$

In Equation (16) u^+ has the same significance as in the pipe flow case, $\xi = y/h$ is the dimensionless position variable (y is measured from the channel centerline), and

$$\phi = \frac{R - R_c}{4b\sqrt{2}} \tag{17}$$

In Equation (17), b has the same significance as before, and

$$R \equiv N_{Re}\sqrt{f} \tag{18}$$

with N_{Re} and f defined as

$$N_{Re} = 4h\rho <v>/\mu \tag{19}$$

$$f = 2\tau_w/\rho <v>^2 \tag{20}$$

so that for laminar flow $fN_{Re} = 24$. For the choice of Reynolds number used here one can easily show (7) that $(N_{Re})_c = 2{,}800$, and hence, $R_c = 2{,}800\sqrt{24/2{,}800} = 259.230$.

By using the same value $a = 60$ for this problem as in the pipe flow case, Gill and Scher (5) were in reality using a value of $R_c = 339.41$, which corresponds to $(N_{Re})_c = 4{,}800$. This value of $(N_{Re})_c$ is greatly at variance with the established (7) value of 2,800.

Equation (16) is clearly quadratic in $(-du^+/d\xi)$ and, as before, may be formally solved to obtain u^+ as

$$u^+ = \frac{2\sqrt{2}}{k^2R}\int_\xi^1 G(k, R, \phi, \xi')d\xi' \tag{21}$$

where

$G(k, R, \phi, \xi) =$

$$\frac{\left\{1+\frac{1}{8}k^2R^2\xi(1-\xi)^2\left[1-\exp(-\phi(1-\xi))\right]^2\right\}^{1/2}-1}{(1-\xi)^2\left[1-\exp\left(-\phi(1-\xi)\right)\right]^2} \tag{22}$$

For this geometry the mean velocity, $<v>$, is given by $u^* \int_o^1 u^+ \ (\xi)d\xi$. Thus, one can write

$$N_{Re}=\frac{2}{k^2}\int_o^1 \int_\xi^1 G(k,R,\phi,\xi')d\xi' \ d\xi \tag{23}$$

The dimensionless velocity profile is given by

$$\frac{v(\xi)}{<v>}=\frac{\int_\xi^1 G(k,R,\phi,\xi')d\xi'}{\int_o^1 \int_\xi^1 G(k,R,\phi,\xi')d\xi' \ d\xi} \tag{24}$$

and the ratio of average to maximum velocity is

$$\frac{<v>}{v_{\max}}=\frac{\int_o^1 \int_\xi^1 G(k,R,\phi,\xi')d\xi' \ d\xi}{\int_o^1 G(k,R,\phi,\xi)d\xi} \tag{25}$$

RESULTS

It is evident, in view of Equations (8) and (17), that selection of the parameter R (for a preselected value of b) determines unique values of N_{Re}, $v(\xi)/<v>$, and $<v>/v_{\max}$ by Equations (13) to (15) and (23) to (25) for the cases of flow in pipes and between parallel plates, respectively. The uniqueness of these results, and their dependence on R is not clear from the paper by Gill and Scher (*5*). In their paper, they presented two figures showing sets of velocity profile curves for both geometries with N_{Re} rather than R appearing as the curve parameter. These curves were actually computed (*8*) by using an empirical $f - N_{Re}$ relation to determine R for a given value of N_{Re}, thus circumventing the integration required by Equations (13) and (23). However, as will be seen shortly, this procedure can lead to considerable error in the transition region for their choice of constants. Therefore, in order to avoid such errors, and to provide a completely theoretical calculation of the $f - N_{Re}$ curve for all Reynolds numbers, the shortcut method (*8*) of Gill and Scher will not be used here.

Equations (13) to (15) and (23) to (25) have been integrated numerically on a digital computer by means of a Gaussian quadrature* procedure (*9*). The results of these integrations are shown in Figures 1 to 6 together with experimental data taken from the numerous literature sources cited thereon. Also, in Figures 1, 2, 4, and 5, are shown as dashed curves the corresponding results computed by the author using the constants of reference 5.

DISCUSSION OF RESULTS

Figure 1 is a plot of the product fN_{Re} as a function of N_{Re} for flow of Newtonian fluids in pipes for the laminar, transitional, and turbulent regimes of flow. The solid curve for $N_{Re} > 2{,}100$ was calculated from Equation (13) with the empirical constant b chosen equal to 22 to achieve agreement with the high Reynolds number data. For $N_{Re} < 2{,}100$, the solid curve is a plot of the Hagen-Poiseuille equation, $fN_{Re} = 16$. The dashed curve in Figure 1 was computed by the author using constants of reference 5.

* Although the Gaussian quadrature formulae are the most accurate (*9*) of the numerical quadrature rules, special care must be exercised in their use with functions of the type encountered here, as is explained in reference *10*.

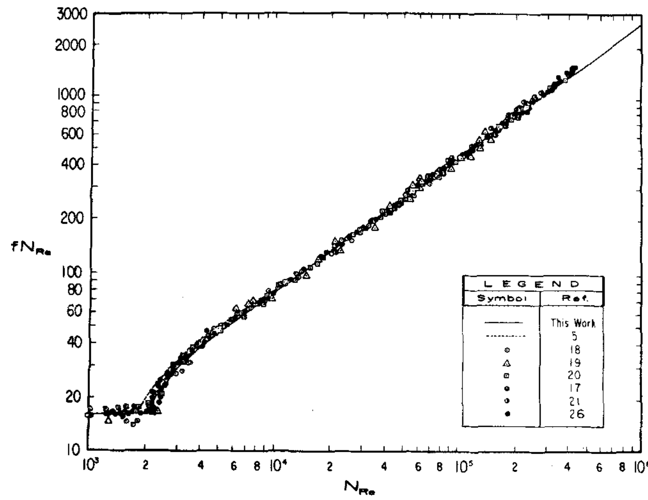

Fig. 1. Product of friction factor times Reynolds number as a function of Reynolds number for isothermal flow of Newtonian fluids in smooth straight pipes of constant circular cross section. Solid curve was calculated from Equation (13). Dashed curve was computed from the constants of reference 5. Experimental data were taken from the sources noted.

It is apparent from Figure 1 that the choice of R_c given by Equation (10) achieves a better representation of the experimental data in the transition region than that obtained previously (*5*).

Gill and Scher (*5*) selected the constant a corresponding to $(N_{Re})_c = 1{,}800$ because (*5*) "the experimental data of Senecal" (*11*) "indicate that the Hagen-Poiseuille equation describes flow in tubes well up to Reynolds number of approximately 1,800." However, Figure 2, which is a plot of $<v>/v_{\max}$ as a function of N_{Re} computed from Equation (15) (solid curve) and which contains the data in question (*11, 12*), clearly shows that $(N_{Re})_c = 2{,}100$ is the correct value to be used. Again, the dashed curve was computed from the constants of reference *5*.

Figure 2 reveals a characteristic of this theory not indicated previously (*5*). Clearly, for $N_{Re} > 3{,}500$ the theoretical value of $<v>/v_{\max}$ lies above the spread of the experimental data. That this was also true of Gill and Scher's results is evident from the fact that the solid and dashed curves merge indistinguishably for $N_{Re} > 6{,}000$.

It is of interest to note that although the theory fails to provide an accurate prediction of $<v>/v_{\max}$, except in the transition range, it does provide an excellent prediction of the product fN_{Re} over the entire range of Reynolds numbers for which data are available.

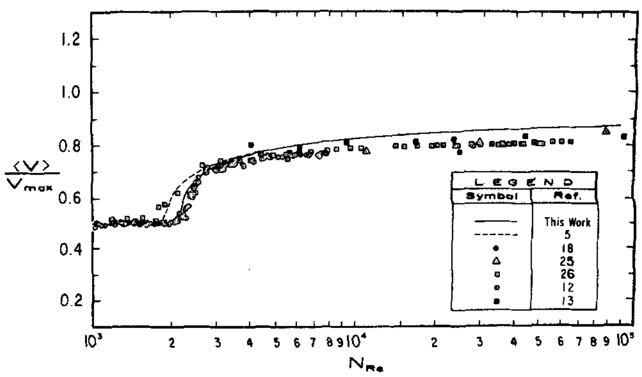

Fig. 2. Ratio of average to maximum velocity as a function of Reynolds number for isothermal flow of Newtonian fluids in smooth straight pipes of constant circular cross section. Solid curve was computed from Equation (15). Dashed curve was computed from the constants of reference 5. Experimental data were taken from the sources noted.

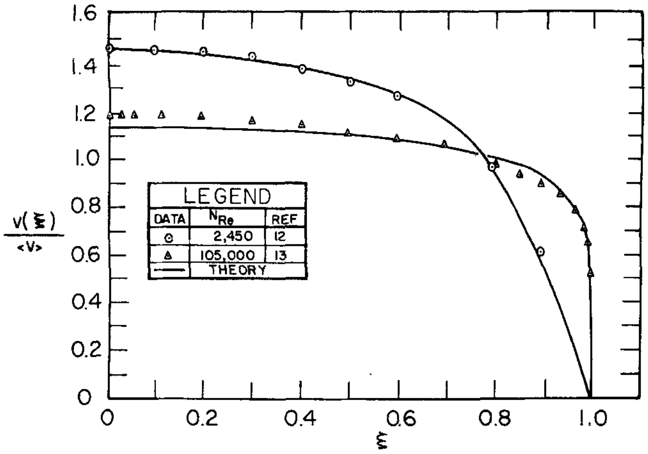

Fig. 3. Ratio of local to average velocity as a function of dimensionless position, r/r_w, for isothermal flow of water in a smooth pipe. Experimental data are those of authors cited. Solid curves were calculated from Equation (14).

Figure 3 is a plot of computed velocity profiles compared with the data of Senecal and Rothfus (*12*) and Nikuradse (*13*) for two widely separated Reynolds numbers. For the transitional range data (*12*) the theory is seen to follow the data fairly well. For the highly turbulent data (*13*), however, the theory crosses the data. In particular, the theoretical curve falls below the data for $\xi < 0.5$.

In the highly turbulent range, the influence of the parameter R_c is no longer significant and the exponential damping factor reduces to that of Van Driest (*4*). The only difference between the present theory at large Reynolds numbers and that of Van Driest (*4*) is the inclusion of the spatial variation of the shear stress which causes the velocity gradient to vanish at the centerline of the duct.

The failure of the present theory to achieve complete success in representing velocity profile data as accurately† as Van Driest's theory (*4*) is due to the inclusion of the spatially variable shear stress term. Evidently, when this variation is retained (as physically it must be in any fully correct theory), the inherent inadequacy of the Prandtl mixing length model to account fully for the details of the mean turbulent flow field is clearly revealed. Even the inclusion of Van Driest's wall damping factor (*4*) is unable to compensate fully for this inherent deficiency. However, since what is desired in many applications is an accurate calculation of the frictional drag resistance, the present theory appears to have adequately averaged the velocity profile inaccuracies so as to produce an accurate frictional resistance curve, and therefore, should prove useful in connection with heat and mass transfer analogy calculations where this wall frictional resistance behavior is all important. Certainly in the transition region very precise results should be obtainable, and even in highly turbulent flow the velocity profiles near the wall are sufficiently precise for accurate heat and mass transfer calculations to be made.

Figure 4 is a plot of the product of fN_{Re} as a function of N_{Re} for flow between parallel planes. The solid curve was computed from Equation (23) with $b = 23$, and the dashed curve was computed by the author from the constants of reference 5. It is clear from Figure 4 that the value of R_c computed theoretically (*7*) provides a much better representation of the transitional flow data‡ than the empirical value used previously (*5*).

Although Gill and Scher proposed using $b = 22$ for both cases, careful examination of Figure 4 reveals that their curve lies somewhat above the present theory for high N_{Re}. A better fit to the data, and coincidence with the present theory, would have been obtained had they used $b = 23$ also. Thus, it appears that different values of the damping coefficient b are required as the surface curvature changes.

Since the present results and those of Gill and Scher (*5*) do not become approximately coincident until $N_{Re} > 2 \times 10^4$, and since the majority of the eigenvalues calculated by Gill and Lee (*14*) for transitional flow heat transfer were for $N_{Re} < 2 \times 10^4$, it would appear that a recalculation of these eigenvalues is in order.

It should be clear from Figure 4 that the shortcut method of computation (*8*) used in the preparation of the velocity profile curves in reference 5 can lead to very serious errors in the transition region, particularly with the choice of empirical constants used therein (*5*). This method should, therefore, be avoided.

Figure 5 is a plot of $\langle v \rangle / v_{max}$ calculated from Equation (25) (solid curve) and from the constants of reference 5 (dashed curve). A curve similar to the dashed one in Figure 5 was discussed qualitatively by Gill and Lee (*14*) without comparison with experimental data. Again the high Reynolds number behavior of the theory is seen

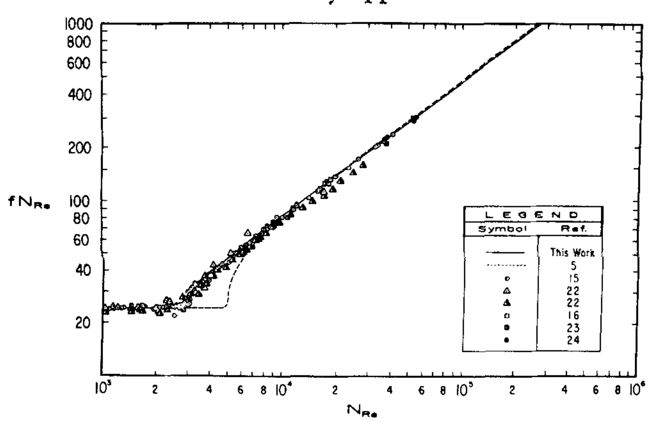

Fig. 4. Product of friction factor times Reynolds number as a function of Reynolds number for isothermal flow of Newtonian fluids in smooth straight ducts of constant rectangular cross section and large aspect ratio approximating infinite parallel planes. Solid curve was computed from Equation (23). Dashed curve was computed from the constants of reference 5. Experimental data were taken from the sources noted.

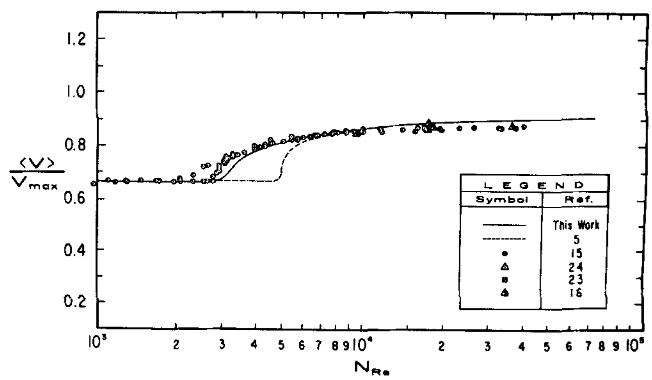

Fig. 5. Ratio of average to maximum velocity as a function of Reynolds number for isothermal flow of Newtonian fluids in smooth straight ducts of constant rectangular cross section and large aspect ratio approximating infinite parallel planes. Solid curve was computed from Equation (25). Dashed curve was computed from the constants of reference 5. Experimental data were taken from the sources listed below.

† Careful examination of Van Driest's paper reveals that his theory likewise fell below the velocity profile data near the center of the pipe.

‡ Note that the data of Washington and Marks (*22*) for their ⅛ in. duct are here shifted upward by 20% uniformly. This was done because their published data in the laminar range closely fit the curve $fN_{Re} = 20$ rather than the theoretical value of 24. No explanation is offered for this behavior. For this reason, these data were given a separate symbol (△) from their other data, and included only for qualitative comparison purposes.

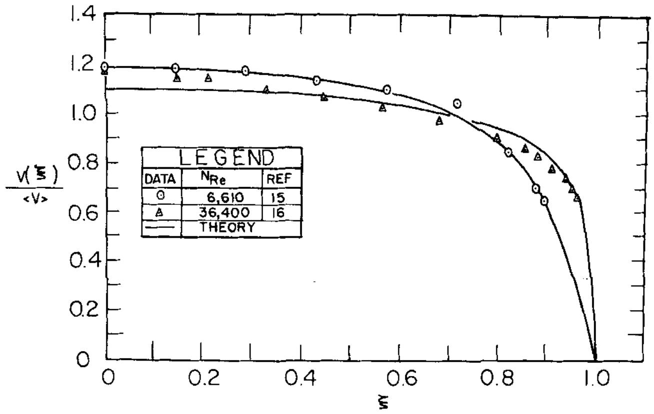

Fig. 6. Ratio of local to average velocity as a function of dimensionless position, y/h, for isothermal flow of water in smooth rectangular ducts of large aspect ratio. Experimental data are those of authors cited. Solid curves were computed from Equation (24).

to be the same as was observed with the pipe flow case. The data shown in the transition region are those of Whan (*15*). It would be desirable to have other data in this region to confirm the apparent discrepancy between the data and theory. It is suspected that if sufficient data were available in this region, scatter similar to that seen in Figures 1 and 4 would be observed and would quite likely include the theory as occurred in the pipe flow case.

Figure 6 is a plot of Whan's velocity profile (*15*) data for $N_{Re} = 6{,}612$ showing the good agreement achieved between the theory and experimental data in the transition region, and the data of Corcoran and coworkers (*16*) for $N_{Re} = 36{,}400$. For the latter data the discrepancy between the theory and experiment at high Reynolds numbers is again apparent.

CONCLUSIONS

The replacement of the empirical constant introduced by Gill and Scher, in their modification (*5*) of Van Driest's (*4*) damping factor for the Prandtl (*1*) mixing-length model of the mean turbulent flow field, by a theoretically calculable parameter (*7*), has been clearly shown to achieve an excellent representation of frictional resistance data. Since heat and mass transfer analogies rely upon accurate values of the friction factor for their success, the present theory clearly offers a considerable possibility of success with heat and mass transfer analogy calculations.

For high Reynolds number flows in both pipes and parallel plane channels, the present theory fails to give an accurate representation of the velocity profile data in the center of the duct. This appears to be due to the inadequacy of the Prandtl mixing-length model, even as modified by Van Driest (*4*) and the present author, to account properly for the variation of the Reynolds stress with position when the variation of the total shear stress with position is taken into account. It therefore appears that further modification of this model is needed if it is to provide a satisfactory description of the entire velocity field. For the transition region, however, the present theory appears to give adequately precise velocity profile curves.

ACKNOWLEDGMENT

A portion of this work was conducted under National Science Foundation Grant No. GK-550 and part was performed by the author while serving as a consultant to the General Electric Company, Hanford Atomic Products Department, Richland, Washington. The numerical computations were performed using the IBM 7040 computer facility at Brigham Young University.

NOTATION

a = constant in Gill and Scher theory
b = Van Driest's damping constant
f = Fanning friction factor
h = half separation distance for parallel plates
k = Prandtl's universal mixing length constant
L = mixing length
N_{Re}^* = parameter defined by Equation (4)
N_{Re} = Reynolds number
R = $N_{Re}\sqrt{f}$
R_c = critical value of R at laminar-turbulent transition
u^+ = v/u^*
u^* = $\sqrt{\tau_w/\rho}$
v = velocity
v_{max} = maximum velocity
$\langle v \rangle$ = area mean velocity
x_j = generalized position variable
y = distance variable
y_m = maximum value of y

Greek Symbols

μ = viscosity of fluid
ξ = dimensionless position variable
ρ = density of fluid
$\tau_{ij}^{(t)}$ = generalized Reynolds stress
τ_w = wall momentum flux

LITERATURE CITED

1. Prandtl, L., *Z. angew. Math. u. Mech.*, **5**, 136 (1925).
2. von Karman, T., *Nachr. Ges. Wiss. Gottingen, Math—physik. Kl.*, (1930); also *Nat. Advisory Comm. Aeron.*, TM 611 (March, 1931).
3. Deissler, R. G., *Natl. Advisory Comm. Aeron., Rept.*, **1210** (1955).
4. Van Driest, E. R., *J. Aeronaut. Sci.*, **23** 1007 (1956).
5. Gill, W. N., and Marvin Scher, *AIChE J.*, **7**, 61 (1961).
6. Bird, R. B., W. E. Stewart, and E. N. Lightfoot, "Transport Phenomena," John Wiley, New York, 1960 Chapt. 5.
7. Hanks, R. W., *AIChE J.*, **9**, 45 (1963).
8. Gill, W. N., private communication (Feb. 13, 1963).
9. Scarborough, J. B., "Numerical Mathematical Analysis," Oxford Univ. Press, London (1955) pp. 145-152.
10. Ralston, Anthony, "A First Course in Numerical Analysis," McGraw-Hill, New York, (1965) pp. 112-113.
11. Senecal, V. E., Ph.D. thesis, Carnegie Inst. Tech., Pittsburgh, Pennsylvania (1952).
12. ———, and R. R. Rothfus, *Chem. Eng. Prog.*, **49**, 533 (1953).
13. Nikuradse, J., *VDI Forschungsheft*, **356** (1932).
14. Gill, W. N., and S. M. Lee, *AIChE J.*, **8**, 303 (1962).
15. Whan, G. A., Ph.D. thesis Carnegie Inst. Tech., Pittsburgh, Pennsylvania (1956).
16. Corcoran, W. H., F. Page, Jr., W. G. Schlinger, and B. H. Sage, *Ind. Eng. Chem.*, **44**, 410 (1952).
17. Walker, J. E., Ph.D. thesis, Carnegie Inst. Tech., Pittsburgh, Pennsylvania (1957).
18. Rothfus, R. R., Ph. D. thesis, *ibid.* (1948).
19. Shaver, R. G., Sc.D. thesis, Mass. Inst. Tech., Cambridge (1957).
20. Dodge, D. W., Ph.D. thesis, Univ. Delaware, Newark (1958).
21. Hanks, R. W., Ph.D. thesis, Univ. Utah, Salt Lake City, (1960).
22. Washington, L., and W. M. Marks, *Ind. Eng. Chem.*, **29**, 337 (1937).
23. Page, F., Jr., W. H. Corcoran, W. G. Schlinger, and B. H. Sage, *ibid.*, **44**, 419 (1952).
24. ———, W. G. Schlinger, D. K. Breaux, and B. H. Sage, *ibid.*, **44**, 424 (1952).
25. Wells, C. S., Jr., J. Harkness, and W. A. Meyer, *LTV Research Center, Report No.* 0-71000/6R-22, Dallas, Texas (Dec. 1966).
26. Stanton, T. E., and J. R. Pannell, *Phil. Trans. Roy. Soc. (London)*, **214A**, 199 (1914).

Manuscript received April 13, 1967; revision received October 23, 1967; paper accepted October 25, 1967. Paper presented at AIChE New York meeting.